29th Congress of the International Council
of the Aeronautical Sciences
St. Petersburg, Russia; September 7-12, 2014

CONCEPTUAL DESIGN OF SOLAR UAV FOR LONG ENDURANCE

Nobuyuki ARAI*, Wail HARASANI and Katsumi HIRAOKA***
***Tokai University, **King Abdulaziz University**

Keywords: *Solar plane, Design, Green power*

Abstract

Solar plane for long endurance is required a restriction of power for flight and high lift force. In this paper, the design method considered about the influence with temperature is explained, and the candidate specification of flyable solar plane for multiple days is introduced.

1 Introduction

The solar plane is under development in order to become commonplace for the purposes, which are platform for radio communication, observation in the nature disaster, flight in atmosphere of Mars and so on for example, because of its long endurance.

In this study, at the first step, we created the prototype solar plane “Sun Falcon1” controlled by radio control which the goal of the design was set to the day flight with auto pilot as shown in Fig.1. Moreover, we are going to develop the solar UAV “SunFalcon2”, which can fly for multiple days under a condition of climate in Saudi Arabia, based on an improved conceptual design procedure.

A serious power balance between supply and consumption is required for multiple-days flight. Moreover, since the weight of the battery which has the capacity to keep flying for night becomes heavy, high lift force is almost required under a minimum power wherever possible. On the other hand, because of being influenced with the temperature, efficiency of solar cell, which varies during a flight in a day, should be estimated in an accurate way. And so, an environment model about temperature and estimation of critical power for multiple-days flight are mentioned as below. And the specification of flyable solar plane for long endurance is led by using a conceptual design procedure considered about these issues.

Fig.1 Test flight of Day-flight Solar Plane “SunFalcon1”

2 Environment Model

2.1 Climate of Jeddah

The daily global horizontal radiation of Jeddah changes throughout the year as a bar chart shown in Fig.2[1]. Maximum and minimum radiations are 7,451[Wh/m^2 day] at June and 4,150[Wh/m^2 day] at December, respectively. The minimum radiation should be used to find whether solar plane can fly all days in the year or not. However, average radiation value, 6,002[Wh/m^2 day], was chosen as the daily global horizontal radiation Rad_{sun} because the minimum value is not enough to fly for multiple days.

Moreover, the distributions of month-by-month highest and lowest temperature are shown by a lines in Fig.2. The highest temperatures of each distribution are 39.4[degrees C] and 27.6[degrees C]. Since the efficiency of solar cell falls down with a rise of temperature, these values are used as highest and lowest temperature in a day, T_{TH} and T_{TL} to set a worse condition for temperature change.

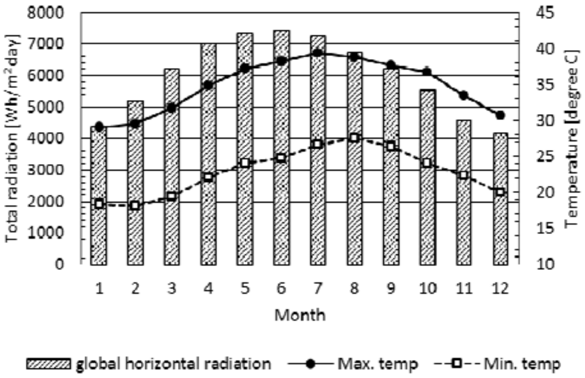

Fig.2 Temperature and Global Horizontal Radiation of Jeddah

2.2 Temperature Model

2.2.1 The temperature on ground

Since efficiency of solar cell is influenced with its temperature, varying efficiency can be obtained by trigonometric function with arbitrary highest and lowest temperature.

$$T_{gound}(\theta) = \frac{T_{TH}+T_{TL}}{2} + \frac{T_{TH}-T_{TL}}{2}\cos\left\{\frac{1}{2-R_b}\left(\theta - \frac{H_{TH}-24}{12}\right)\pi\right\} \quad (0 \le \theta < \theta_{TL})$$

$$T_{gound}(\theta) = \frac{T_{TH}+T_{TL}}{2} - \frac{T_{TH}-T_{TL}}{2}\cos\left\{\frac{1}{R_b}\left(\theta - \frac{H_{TL}}{12}\right)\pi\right\} \quad (\theta_{TL} \le \theta < \theta_{TH}) \qquad (1)$$

$$T_{gound}(\theta) = \frac{T_{TH}+T_{TL}}{2} + \frac{T_{TH}-T_{TL}}{2}\cos\left\{\frac{1}{2-R_b}\left(\theta - \frac{H_{TH}}{12}\right)\pi\right\} \quad (\theta_{TH} \le \theta \le 2\pi)$$

The curve of temperature which changes in a day is approximately obtained as shown in Fig.3 by using H_{TL} =300.7[K] at 6 a.m. and T_{TH}=312.5[K] at 2 p.m. in this example.

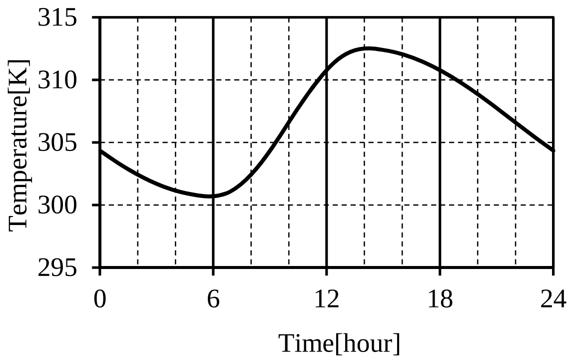

Fig.3 Temperature on Ground in a Day by the Model

2.2.2 The temperature, pressure and density in the midair

Temperature, pressure and density at arbitrary altitude can be determined by

$$T_{midair} = \mathrm{T}_{\mathrm{ground}} + \Delta T * h \qquad (2)$$

$$p_{midair} = p_{ground}\left(T_{midair}/T_{ground}\right)^{\frac{g}{-\Delta T\,R}} \qquad (3)$$

$$\rho_{midair} = \rho_{ground}\left(T_{midair}/T_{ground}\right)^{\left(\frac{g}{-\Delta T\,R}-1\right)} \qquad (4)$$

where ΔT is the lapse rate of atmospheric temperature, -0.00649[K], and h represents altitude.

3 Model of Solar Plane

3.1 Efficiency Model of Solar Module

The general efficiency of the monocrystalline silicon solar cell at 300[K] is estimated as 20% by taking consideration the state that the dust like sand over the surface of solar module blocks the shine of the sun.

3.1.1 Dependence on the environment temperature

Actual efficiency of solar module is influenced with atmospheric temperature and radiation heat. The atmospheric temperature can be estimated by temperature on the ground and altitude of plane.

Actual efficiency of solar module μ_{solm} can be represented by an efficiency of solar module at 300[K]. μ_{m} and lapse rate of solar cell for the temperature of cell μ_{rate} as

$$\mu_{solm} = \mu_m + \mu_m\mu_{rate}\left(T_{ground} + \Delta T\cdot h\right) \qquad (5)$$

By considering that T_{ground} and h are the function of time θ in nature,

$$\mu_{solm}(\theta) = \mu_m + \mu_m\mu_{rate}\left[T_{ground}(\theta) + \Delta T\{h_{low} + dh(\theta)\}\right] \qquad (6).$$

3.1.2 The model of power supplied by solar module

When the change of power supplied by solar module in a day is replaced with the trigonometric function approximately as shown in Fig.4, maximum power can be obtained from above mentioned daily global horizontal radiation by similarity rule of area.

An area density of maximum power which solar module can receive p_{max} can be obtained as

$$p_{max} = \frac{Rad_{sun}}{(2 \times 12)}\pi \qquad (7)$$

where Rad_{sun} is area density of daily global horizontal radiation as shown in Fig.4.

3.2 Estimation of Desired Power for Flight

3.2.1 Characteristics of main wing

Since an airfoil of the plane for long duration needs high lift-drag ratio, wing section of glider is agreeable. Then SD7037 airfoil[2] was the chosen as templa0te of wing section because of high lift-drag force and stability of performance for lift and drag. To use for conceptual design calculation, approximation formula of C_L for two dimensional wing is obtained as linear function,

$$C_{L_{2d}}(\theta) = 5.962\frac{(\alpha - \alpha_0)}{180}\pi \qquad (8),$$

where zero-lift attack angle $\alpha_0 = -3[degrees]$.

Reynolds number effect doesn't be considered for simplification because C_L distribution of SD7037 airfoil is almost same in high Reynolds number field.

Additionally, in this conceptual design calculation, the monoplane equation[3] was used to obtain a lift coefficient of three dimensional wing $C_{L_{3d}}$ with different aspect ratio and taper ratio.

Drag coefficient for main wing is estimated by incorporating friction coefficient and induced drag coefficient. Friction coefficient in laminar and turbulent flow can be represented as

$$C_{f\,laminar} = \frac{1.328}{\sqrt{Re}} \qquad (9)$$

$$C_{f\,tubulance} = \frac{0.455}{(\log_{10} Re)^{2.58}} \qquad (10).$$

Total of friction coefficient is represented by

$$C_f = C_{f\,turbulance} - \frac{x_{tr}b}{S_w}\left(C_{f\,turbulance} - C_{f\,laminar}\right) \qquad (11)$$

Where x_{tr} is the transition point to turbulence from laminar which is estimated by

$$x_{tr} = \frac{3.0 \times 10^5}{Re}c \qquad (12).$$

And the induced drag coefficient C_{D_i} of three dimensional wing can be obtained by the monoplane equation with difference of aspect ratio and taper ratio. Drag coefficient of wet area of whole plane can be expressed by

$$C_D = \left(2.6C_f + C_{D_i}\right)/(1 - 0.15) \qquad (13)$$

where 2.6 means the rate of wet area for wing are, and 0.15 represents the rate of profile drag and interference drag for total drag.

3.3 Required Power for Flight

The relation of forces which act on plane is

$$T = D + W\sin\alpha \qquad (14)$$

$$L = W\cos\alpha \qquad (15).$$

Thrust is represented by lift and drag as

$$T = D + L\tan\alpha \qquad (16),$$

then, power for flight is obtained by

$$\begin{aligned} P &= TV \\ &= DV + LV\tan\alpha \\ &= \frac{1}{2}\rho V^3 C_D S_w + \frac{1}{2}\rho V^3 C_L S_w \tan\alpha \end{aligned} \qquad (17).$$

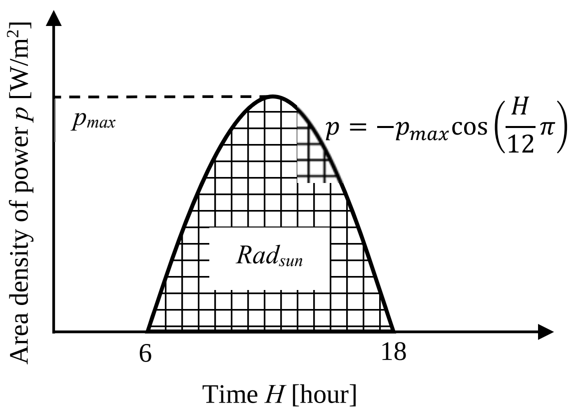

Fig.4 Trigonometric Distribution of Supplied Power

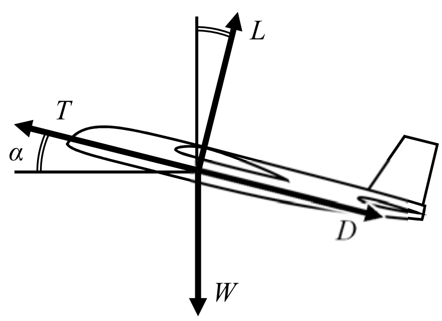

Fig.5 Forces Acting for Airplane

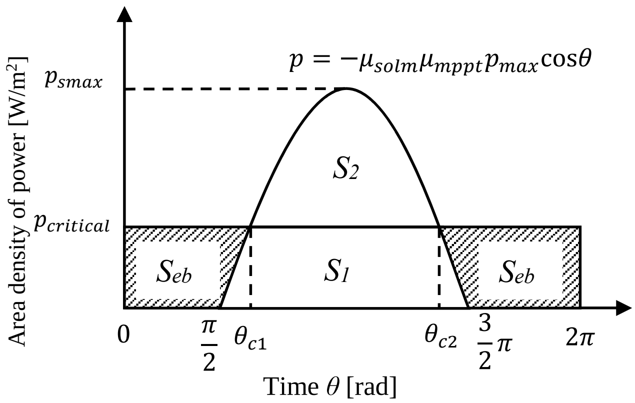

Fig.6 Required Energy for Night-time Flight

3.4 Critical Power for Multiple-day Flight

An energy that solar modules supplies is expended as the one for flight. The energy for night-time flight should be charged during day-time flight, and paid by a surplus energy that doesn't be used in day-time flight.

In Fig.6, area S_{eb}, S_1 and S_2 show the energy for night-time flight, the one of day-time flight and the surplus energy of day-time, respectively. And $p_{smax} = \mu_{solm}\mu_{mppt}p_{max}$ if μ_{solm} is constant.

The maximum power needed for flight with constant velocity and altitude in a day has a limitation which satisfies a restriction that

$$S_{eb} \le S_2 \qquad (18).$$

By solving the relation

$$2\int_{\frac{\pi}{2}}^{\theta_{c1}} \{p_{critical} - (-p_{smax}\cos\theta)\}\, d\theta + p_{critical}\pi \qquad (19),$$

$$= \int_{\theta_{c1}}^{2\pi-\theta_{c1}} (-p_{smax}\cos\theta - p_{critical})\, d\theta$$

a critical power $p_{critical}$ can be obtained as

$$p_{critical} = \frac{1}{\pi}p_{smax} \simeq 0.318 p_{smax} \qquad (20).$$

Therefore, under the condition of cruising flight with keeping constant velocity, the solar plane should fill a power condition

$$\frac{P/S_c}{p_{smax}} \le 0.318 \qquad (21)$$

to fulfill the multiple-days flight at least. In this conceptual design calculation, this limitation was used for power restriction for flight, and μ_{solm} is treated as a function of time.

3.5 Minimum Battery Capacity

To estimate a minimum battery capacity, S_{eb} need to be calculated for the power for flight P. When $p_{critical}$, θ_{c1} and θ_{c2} are replaced to p, θ_1 and θ_2, respectively,

$$\begin{aligned} S_{eb} &= \frac{P/S_c}{p_{max}}\theta_1 + \frac{P/S_c}{p_{max}}(2\pi - \theta_2) \\ &- \int_{\frac{\pi}{2}}^{\theta_1} -\mu_{mppt}\mu_{solm}(\theta)\cos\theta\, d\theta \qquad (22), \\ &- \int_{\theta_2}^{\frac{3}{2}\pi} -\mu_{mppt}\mu_{solm}(\theta)\cos\theta\, d\theta \end{aligned}$$

where S_c is the area of solar cells. θ_1 and θ_2 need to be led by solving the relation

$$p = -\mu_{mppt}\mu_{solm}(\theta)\cos\theta$$

preliminarily.

Then a minimum battery capacity can be obtained as

$$E_{b_{min}} = \frac{Rad_{sun}}{2}S_{eb}S_c \qquad (23).$$

If the energy always remains 20% of capacity, a required battery capacity E_b is

$$E_b = E_{b_{min}}/0.8 \qquad (24).$$

3.6 Mass Prediction

Mass of battery M_{bat} and solar module M_{solm} are obtained by

$$M_{Bat} = R_{mass_{Bat}}E_b \qquad (25)$$

$$M_{Solm} = R_{mass_{Solm}}S_c \qquad (26),$$

where $R_{mas_{Bat}}$ and $R_{mass_{Solm}}$ are mass rate of battery and solar modules as Table2.

Then total mass is predicted by

$$M_{Total} = M_{Bat} + M_{Solm} + M_{af} + M_{payload} \qquad (27)$$

where M_{af} means mass of airframe and includes motor, gear and so on.

To predict the mass of airframe, relation formula which is supposed by Noth[4] was used in this program.

$$M_{af(Noth)} = 0.44b^{3.1}AR^{-0.25}/g \qquad (28).$$

This relation was led statistically from manned gliders and radio controlled plane.

4 Simulation method

Flow chart shown in Fig.7 was repeated for each condition of aspect ratio, taper ratio, span, and velocity. Most of calculation is algebraic formula except for determining of θ_1, θ_2, θ_{c1} and θ_{c2}. These values are determined by the iterative calculation which is Newton-Raphson method. Variables changes in this calculation as shown in Table1. And judgment whether the plane of each case can fly or not was performed after all condition was calculated. Table2 shows efficiencies and mass rate. Value of $R_{mass\,Bat}$ is based on a specification of lithium-ion battery.

5 Result

Fig.8 shows the distributions of power per unit are for variable aspect ratio and velocity when span b = 4 [m]. Critical power per unit area is constant. It is clear that the cruising velocity increases, the more required power almost increases. Additionally, each curve are distorted due to the difference of friction drag between laminar and turbulent flow region, therefore, there is a minimum value of power per unit area at a specific aspect ratio on each velocity.

Table1 Changed of Calculation Condition

	Range	Step
Taper ratio	0.6 - 1.0[-]	by 0.2 [-]
Aspect ratio	1 - 50 [-]	by 1 [-]
Span	1 - 30 [m]	by 1 [m]
Velocity	10 - 80 [km/h]	by 5 [km/h]

Table2 Fixed Efficiencies and Mass Rate

μ_{prop}	Efficiency of propeller	0.8
μ_{motor}	Efficiency of motor	0.85
μ_{ESC}	Efficiency of speed controller	0.9
μ_{mppt}	Efficiency of MPPT	0.96
μ_m	Efficiency of solar module at 300K	0.2
$R_{mass\,Solm}$	Solar module mass ratio	1.3 [kg/m²]
$R_{mass\,Bat}$	Battery mass ratio	0.005 [kg/(W*hour)]

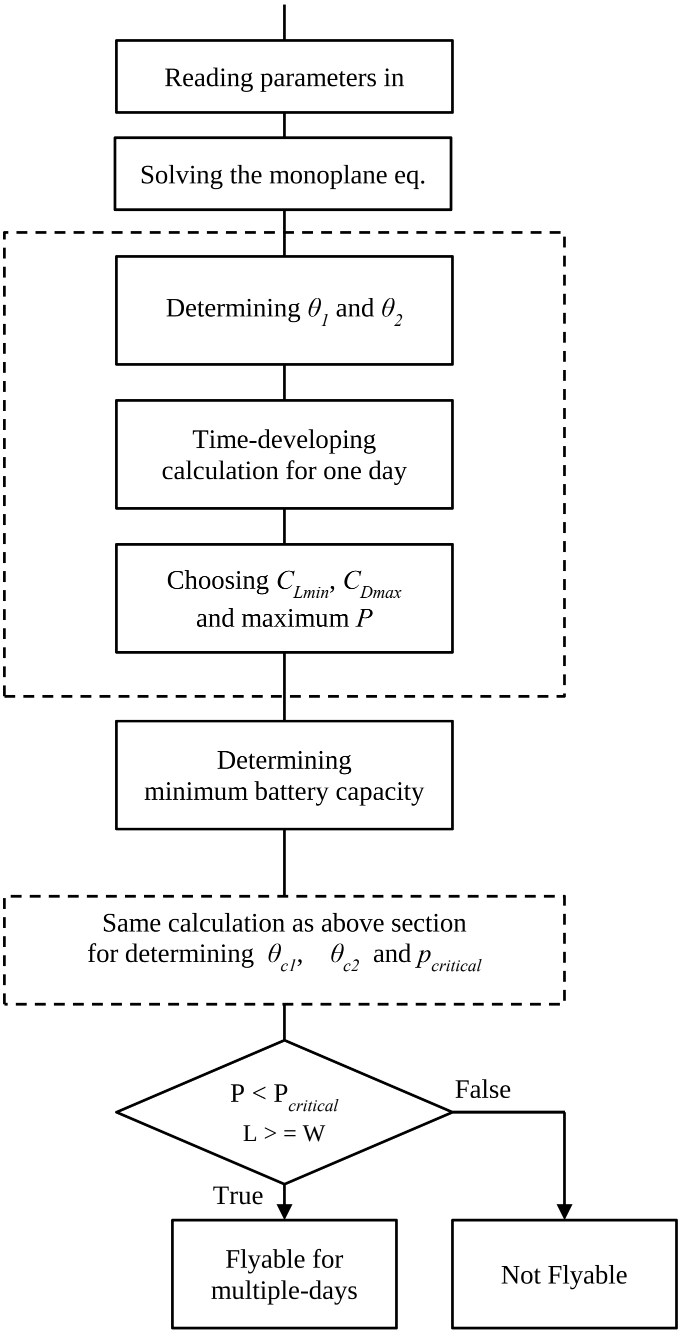

Fig.7 Flow chart for arbitrary conditions (span, aspect ratio, taper ratio and velocity)

Fig.9 shows the weight and minimum Lift distribution with various aspect ratio when span b=4[m] and $M_{af} = 0.55M_{af(Noth)}$. It is clear that the more aspect ratio increases, the more minimum lift and predicted weight decrease, and the range that minimum lift is more than weight is narrow.

Fig.10 shows the region of flyable when span b = 4[m] and $M_{af} = 0.55M_{af(Noth)}$. Blue and orange region represents the filling the flyable condition for power and Lift, respectively.

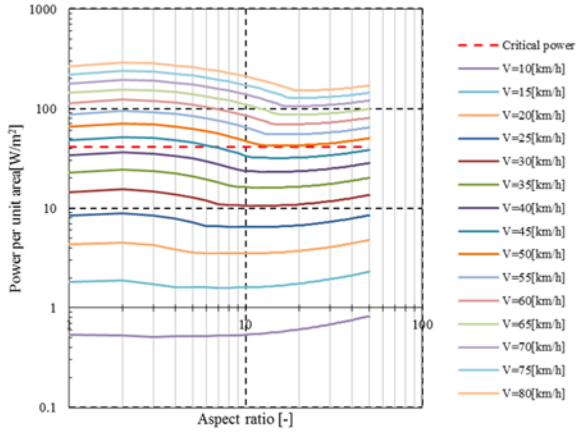

(b=4[m], TR=1, C_{L_2D} =0.6, AoA=0[deg], V=10-80[km/h])

Fig.8 Power Distribution with Various Aspect Ratio

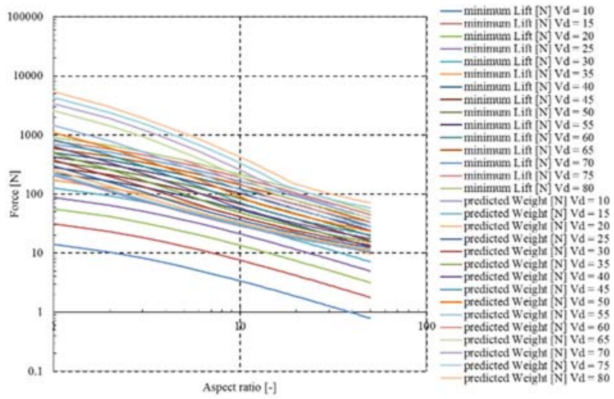

(b=4[m], TR=1, C_{L_2D} =0.6, AoA=0[deg], V=10-80[km/h])

Fig.9 Weight and Minimum Lift Distribution with Various Aspect Ratio

Then, green region shows the region which both condition is satisfied. The plane, which have the specification in this region, can fly for multiple days. The region which satisfies $Lift \geq Weight$ exist like a island because the more the velocity increases, the more the battery weight increase due to the increase of necessary capacity for a flight during night.

The result mentioned above is one in all 136 results which based on other span length, taper ratio or C_L. Actually, number of a square that is indicated by a velocity and aspect ratio, colored by green, of flyable condition is 161 at $C_{L(2D)} = 0.6$, and 1,218 at $C_{L(2D)} = 0.8$ as shown in Table 3. However, many results that the weight of airframe is too light are included in

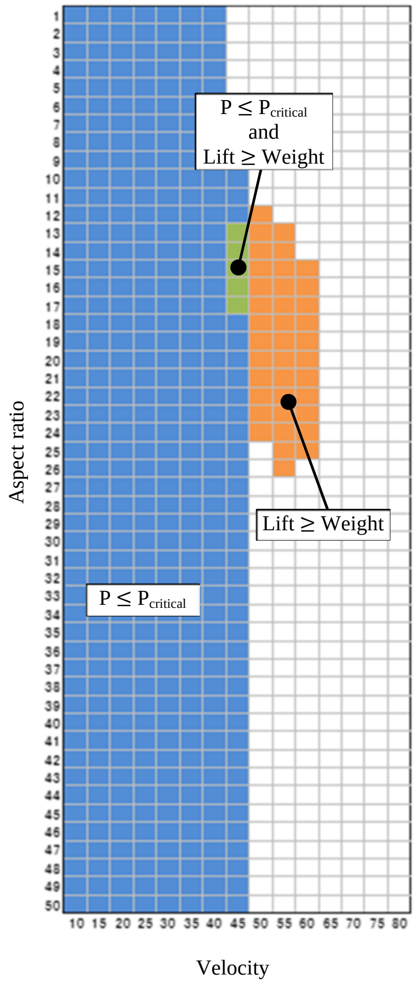

(b=4[m], TR=1, C_{L_2D} =0.6, AoA=0[deg], V=10-80[km/h])

Fig.10 Region of the Flyable Condition for Multiple Days

these case. It is difficult to make the airframe which have enough stiffness to sustain its structure under those conditions. So, to find whether the weight of airframe is enough or not, Noth's weight prediction formula is used as

$$Lift_{min} - (W_{Bat} + W_{Solm}) \geq M_{af(Noth)} \qquad (29)$$

If this condition is filled, it is clear that the plane have enough lift force to carry the weight of airframe with the sufficient stiffness. The cases which satisfied this result is nothing at $C_{L(2D)} = 0.6$, and just 84 cases at $C_{L(2D)} = 0.8$ as shown in Table3.

Finally, the specifications of the 84 cases are limited as shown in Table4.

Table3 Number of Cases for Flyable and Maufacturable

$C_{L(2d)}$	Flyable	Manufacturable
0.6	161 cases	0 cases
0.8	1,218 cases	84 cases

Table4 Specification of Flyable and Manufacturable Plane

Span [m]	AR [-]	TR [-]	Velocity [km/h]	Mass [kg]
2	15-20	1.0	40	1.2
2	13-24	0.8	40	1.4-0.8
2	12-26	0.6	40	1.5-0.8
2	11-28	0.4	40	1.7-0.7
3	13-19	0.6	40	3.3-2.3
3	12-21	0.4	40	3.6-2.2
4	18	0.8	45	5.5
4	17-22	0.6	45	5.8-4.7
4	16-24	0.4	45	6.3-4.3

6 Conclusion

By using a conceptual design method which included an influence of temperature and critical power for cruising flight, the candidates of specification of solar plane can be obtained.

References

[1] A.A. El-Sebaii, F.S. Al-Hazmi, A.A. Al-Ghamdi, S.J. Yaghmour, Global, direct and diffuse solar radiation on horizontal and tilted surfaces in Jeddah, Saudi Arabia, Applied Energy, Volume 87, Issue 2, February 2010, Pages 568–576, Elsevier

[2] MichaelS. Selig, James J. Guglielmo, Andy P. Broeren and Philippe Giguere, Summary of Low-Speed Airfoil Data, Volume 1, p.217, SoarTech Publications

[3] Glauert, H., The elements of aerofoil and airscrew theory. Cambridge University Press, 1983

[4] Andre Noth, Design of Solar Powered Airplanes for Continuous Flight, p.47, ETH Zurich, 2008

Acknowledgment

This project was founded by deanship of scientific research (DSR) KingAbdulaziz University, Jeddah, under the grant No. (431/009), the authors, therefore, acknowledge with thanks DSR technical and financial support, furthermore the authors would like to express their gratitude and appreciation to Tokai University for their technical help and support.

Copyright Statement